

# Desorption and Electrical Conductivity Studies of Indium Tin Oxide Powders and Thick Films <sup>†</sup>

Stefan Dietrich \* and Mihails Kusnezoff

Fraunhofer Institute for Ceramic Technologies and Systems IKTS, 01277 Dresden, Germany;  
mihails.kusnezoff@ikts.fraunhofer.de

\* Correspondence: stefan.dietrich@ikts.fraunhofer.de; Tel.: +49-351-2553-7880

<sup>†</sup> Presented at the Eurosensors 2018 Conference, Graz, Austria, 9–12 September 2018.

Published: 21 December 2018

**Abstract:** The influence of various gas compositions on surface adsorbate species and electrical conductivity of indium tin oxide (ITO) powders and thick films was studied. By combining results of temperature dependent desorption (TPD) with electrical conductivity measurements it was shown that, after exposure to ambient air, the surfaces of both powders and films are covered with significant amounts of oxygen, water and carbon related species. While the influence of oxygen adsorbates has already been described for temperatures below 500 °C, desorption of some of these species could be detected at temperatures as high as 675 °C, with a significant influence on electrical film conductivity.

**Keywords:** gas sensor; indium tin oxide; desorption

## 1. Introduction

Indium tin oxide (ITO) is a promising candidate for employment as sensitive layer in various types of gas sensors. While ITO thin films have been extensively studied during the past decades [1–3], little information is available regarding its use in porous thick films, particularly at  $T > 500$  °C [4]. To investigate ITO-gas interactions in a wider temperature range, TPD measurements on nanoscale ITO powders have been carried out at RT–700 °C and compared to electrical conductivity measurements of screen printed and fired ITO thick films.

## 2. Materials and Methods

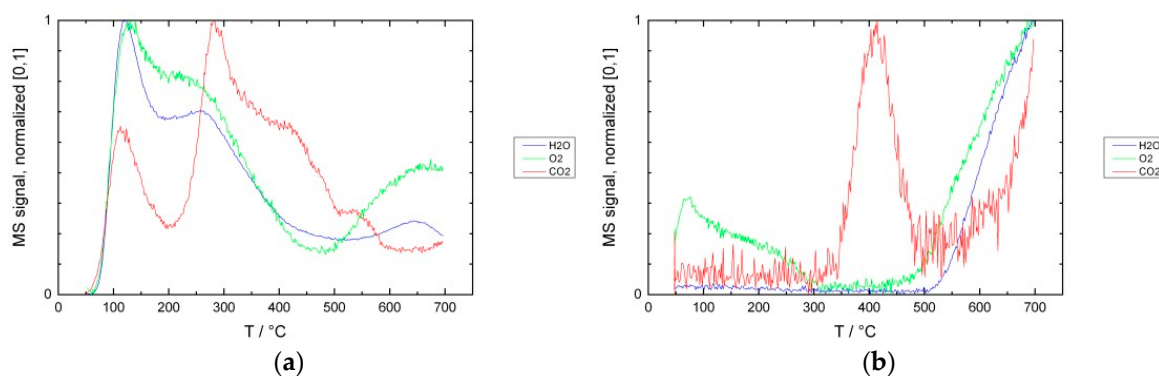
Temperature programmed desorption (TPD) measurements have been carried on commercial ITO powders (Inframat Advanced Materials, USA) in a AutoChem II 2920 System (Micromeritics Instrument Corp., GA, USA) equipped with a ThermoStar GSD 301 T1 quadrupole MS (Pfeiffer Vacuum GmbH, Germany). TPD measurements were performed in both He and He with 12.5 vol% O<sub>2</sub> at RT–700 °C with a heating rate of 10 K/min. Qualitative analysis of MS signals was limited to gas species showing relevant signals (O<sub>2</sub>, H<sub>2</sub>O, CO<sub>2</sub>). For electrical conductivity studies, thick film pastes were prepared from the ITO powder and screen printed onto 3YSZ substrates (Kerafol GmbH, Germany), with pre-deposited Au thick film contacts. The ITO films were fired at 700 °C in air, the resulting porous films are  $7 \times 2$  mm<sup>2</sup> in size, with a thickness of 10 µm. For the measurement of the electrical film properties, samples were placed in a sample holder within a tube furnace, electrical connections were made using Au wires and paste. Gas composition was adjusted using mass flow controllers (Bronkhorst High-Tech B.V., The Netherlands), while a type 2400 source meter (Keithley Instruments / Tektronix, Inc., OR, USA) was used to record resistance. To obtain precise temperature readings during measurement, a Type-S thermocouple was placed close to the sample, which was read out using an Almemo 2390-3 data logger unit (Ahlborn Mess- und Regelungstechnik, Germany).

The measurements were performed in N<sub>2</sub> using the same temperature range and heating rate as the TPD measurements (RT–700 °C, 10 K/min).

### 3. Results

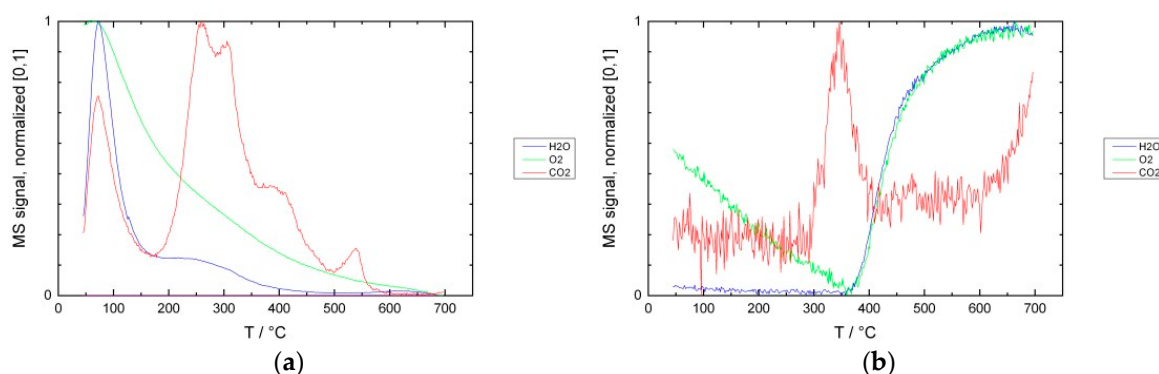
#### 3.1. Desorption Measurements

Figure 1 shows two TPD spectra of ITO powder recorded in He. To aid in readability, mass spectrometer signals for O<sub>2</sub>, H<sub>2</sub>O and CO<sub>2</sub> are normalized. Spectrum (a) was acquired after powder exposure to ambient air for 1 h, spectrum (b) directly after spectrum (a). In spectrum (a), all gases exhibit a large peak at 115–130 °C, one additional peak is observed for O<sub>2</sub> at 670 °C. H<sub>2</sub>O shows additional peaks at 260 and 640 °C, while a large CO<sub>2</sub> peak can be found at 290 °C with further peaks at 410 and 530 °C. In the second measurement (Figure 1b), CO<sub>2</sub> is detected at 410 °C, while the signal of all species shows a steep increase at T > 500 °C.



**Figure 1.** TPD in He after exposure to ambient air (a), subsequent measurement (b).

TPD results in He + 12.5 vol% O<sub>2</sub> show a similar picture (Figure 2): After exposure to ambient air (a), H<sub>2</sub>O shows a peak at 75 °C, while CO<sub>2</sub> peaks are detected at 70, 260–310 and 540 °C. The O<sub>2</sub> signal is only plotted for completeness and shows drift but no desorption. In (b), a CO<sub>2</sub> peak is visible at 350 °C, while signals for O<sub>2</sub> and H<sub>2</sub>O increase rapidly at 370 °C, reaching a shallow peak at 660 °C.

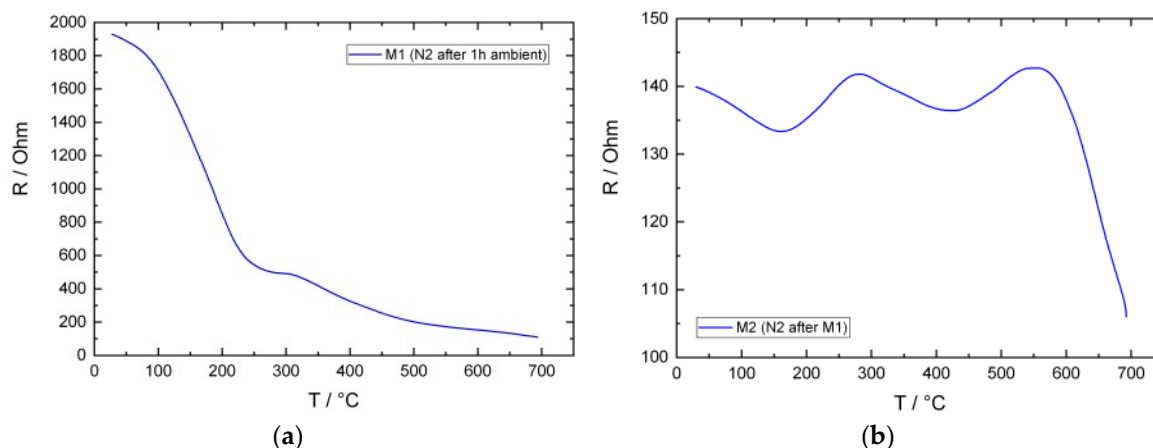


**Figure 2.** TPD in He + 12.5 vol% O<sub>2</sub> after exposure to ambient air (a), subsequent measurement (b).

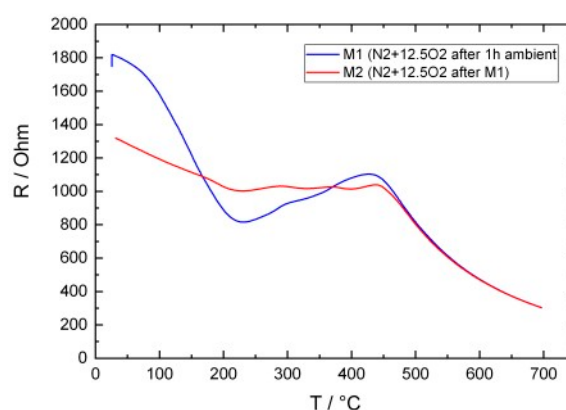
#### 3.2. Electrical Conductivity Measurements

Figure 3 shows R(T) plots recorded for an ITO thick film in N<sub>2</sub>. Plot M1 was obtained after exposure to ambient air for 1 h, M2 (Figure 3b) was recorded immediately after M1. M1 shows a sharp drop in resistance between RT and 250 °C, followed by a shallow decrease towards higher temperatures. In the subsequent measurement (M2), resistance at RT is only slightly higher than at 700 °C in the previous measurement. When the temperature is ramped up, R exhibits four local extrema, before sharply dropping at 570 °C. In Figure 4, R(T) in N<sub>2</sub> + 12.5 vol% O<sub>2</sub> is plotted. Measurement M1 was performed after exposure to ambient air (1 h), M2 immediately after M1.

Although resistance in M1 again shows a steep drop between RT and 220 °C, the relative change is considerably lower than in N<sub>2</sub>. Furthermore, after reaching a local minimum at 220 °C, R increases again until it reaches a local maximum at 420 °C, before dropping off at higher temperatures. In the second measurement, R again decreases to a local minimum at 220 °C but remains almost constant until decreasing beyond 450 °C.



**Figure 3.** R(T) in N<sub>2</sub> after exposure to ambient air (a), subsequent measurement (b).



**Figure 4.** R(T) in N<sub>2</sub> + 12.5 vol% O<sub>2</sub> after exposure to ambient air and subsequent measurement.

#### 4. Discussion

There is ample evidence that ITO surfaces are host to a variety of gaseous species often adsorbed during exposure to ambient air, the most abundant of which are O<sub>2</sub><sup>2-</sup>, O<sub>2</sub><sup>-</sup> and O<sup>-</sup> [5] as well as H<sub>2</sub>O, OH and [OH]<sup>-</sup> groups [6,7]. The TPD spectra for O<sub>2</sub> and H<sub>2</sub>O support these findings, with the majority of these species desorbing between room temperature and 300 °C. While the H<sub>2</sub>O peak at 640 °C suggests residual OH-groups even at this high temperature, the O<sub>2</sub> peak at 670 °C could as well be a result of ITO reduction.

Oxygen chemisorption on ITO proceeds via three possible pathways, all of which have in common that electrons are withdrawn from the oxide surface, resulting in an increase in electrical resistance [5]. During oxygen desorption, on the other hand, electrons are transferred back into the material. In this light, the sharp drop in film resistance observed in both N<sub>2</sub> and N<sub>2</sub> + 12.5 vol% O<sub>2</sub> below 250 °C is consistent with the desorption of oxygen species found in the TPD measurement. While the sharp increase in O<sub>2</sub> signal during the second measurement in N<sub>2</sub> was first thought to be an artifact, the corresponding resistance decrease in the same temperature region supports the hypothesis of further oxygen loss. The resistance decrease in N<sub>2</sub> + O<sub>2</sub> after exposure to ambient air is considerably smaller, and it is assumed that this is because desorbed oxygen is partially replaced by gas phase oxygen. Again, when oxygen desorption increases in the second measurement, resistances drops accordingly.

According to literature it can be assumed that H<sub>2</sub>O chemisorption on ITO is a dissociative process leading to a formation of surface hydroxyl species with an increase in electrical conductivity [3]. In most of our TPD studies, H<sub>2</sub>O desorption is accompanied by O<sub>2</sub> desorption and a significant drop in resistance, which suggests that the resistance increase during H<sub>2</sub>O desorption is outweighed by the resistance decrease due to the desorption of oxygen, which is assumed to be more abundant on the ITO surface. However, during TPD in N<sub>2</sub> + 12.5 vol% O<sub>2</sub>, where the influence of oxygen desorption on resistance is assumed to be lower, resistance still decreases even when strong H<sub>2</sub>O desorption is observed. Currently, no coherent explanation is at hand for these findings and further studies need to be carried out to help understanding the underlying effects.

A few groups have reported on carbon related contaminations found on ITO surfaces [8], however, most authors have been vague about the nature and origin of these species. Their XPS measurement findings have been attributed to graphitic carbon, various hydrocarbons (HCs) and carbon oxides, while other researchers have reported surface carbonate species [9]. It appears reasonable to assume that graphitic carbon and HC species may be residues of solvents or organic compounds used during the ITO powder manufacturing. On the other hand, carbon oxides, and to a lesser extent HCs, may also adsorb during storage and handling of the material in various environments, particularly in ambient air. Considering the fact that complete oxidation of most HCs requires temperatures of at least 150 °C even with effective catalysts [10], it is assumed that the low temperature CO<sub>2</sub> peak found in the TPD spectra can be attributed to CO<sub>2</sub> previously adsorbed from ambient air. The coincidence of the onset of the large CO<sub>2</sub> peak at 300 °C with a steeper drop of the O<sub>2</sub> signal, on the other hand, could be an indication of increasing oxidation of residual HCs and related surface contaminants. Neither of the prominent CO<sub>2</sub> peaks has an obvious representation in the R(T) plots. The dip in resistance for the second measurement in N<sub>2</sub> at 410 °C, however, may be correlated to additional oxygen consumption during oxidation of carbon related species.

**Author Contributions:** S.D. and M.K. conceived the test procedure, S.D. conducted electrical measurements as well as data analysis and wrote the paper.

**Acknowledgments:** No funding was received for the research work presented in this paper.

**Conflicts of Interest:** The authors declare no conflict of interest.

## References

1. Mbarek, H.; Saadoun, M. Screen-printed Tin-doped indium oxide (ITO) films for NH<sub>3</sub> gassensing. *Mater. Sci. Eng. C* **2006**, *26*, 500–504, doi:10.1016/j.msec.2005.10.037.
2. Patel, N.G.; Makhija, K.K. Fabrication of carbon dioxide gas sensor and its alarm system using indium tin oxide (ITO) thin films application. *Sens. Actuators B* **1994**, *21*, 193–197, doi:10.1016/0925-4005(94)01247-4.
3. Yadav, B.C.; Kaushlendra, A. Fabrication and characterization of nanostructured indium tin oxide film and its application as humidity and gas sensors. *J. Mater. Sci. Mater. Electron.* **2016**, *27*, 4172–4179, doi:10.1007/s10854-016-4279-x.
4. Kale, G.M. Solid-state mixed-potential sensor employing tin-doped indium oxide sensing electrode and scandium oxide-stabilised zirconia electrolyte. *Adv. Powder Technol.* **2009**, *20*, 426–431, doi:10.1016/j.appt.2009.09.005.
5. Madhi, I.; Meddeb, W. Effect of temperature and NO<sub>2</sub> surface adsorption on electrical properties of screen printed ITO thin film. *Appl. Surf. Sci.* **2015**, *355*, 242–249, doi:10.1016/j.apsusc.2015.07.135.
6. Donley, C.; Dunphy, D. Characterization of Indium-Tin Oxide Interfaces Using X-ray Photoelectron Spectroscopy and Redox Processes of a Chemisorbed Probe Molecule: Effect of Surface Pretreatment Conditions. *Langmuir* **2002**, *18*, 450–457, doi:10.1021/la011101t.
7. Afshar, M.; Preiss, E.M. Indium-tin-oxide single-nanowire gas sensor fabricated via laserwriting and subsequent etching. *Sens. Actuators B* **2015**, *215*, 525–535, doi:10.1016/j.snb.2015.03.067.
8. Chaney, J.A.; Koh, S.E. Surface chemistry of carbon removal from indium tin oxide by base and plasma treatment, with implications on hydroxyl termination. *Appl. Surf. Sci.* **2003**, *218*, 258–266, doi:10.1016/S0169-4332(03)00617-2.

9. Detweiler, Z.; Wulfsberg, S.N. The oxidation and surface speciation of indium and indium oxides exposed to atmospheric oxidants. *Surf. Sci.* **2015**, *684*, 295–300, doi:10.1016/j.susc.2015.10.026.
10. Zhang, Z.; Jiang, Z. Low-temperature catalysis for VOCs removal in technology and application: A state-of-the-art review. *Catal. Today* **2016**, *264*, 270–278, doi:10.1016/j.cattod.2015.10.040.



© 2018 by the authors. Licensee MDPI, Basel, Switzerland. This article is an open access article distributed under the terms and conditions of the Creative Commons Attribution (CC BY) license (<http://creativecommons.org/licenses/by/4.0/>).